

Title:

Application of Poisson Surface Reconstruction with Envelope Constraints to TLS Point Clouds of Scenes with Complex Objects

Authors:

Daiki Koyama, hmd010205@eis.hokudai.ac.jp, Hokkaido University

Hiroaki Date, hdate@ist.hokudai.ac.jp, Hokkaido University

Satoshi Kanai, kanai@ssi.ist.hokudai.ac.jp, Hokkaido University

Keywords:

Terrestrial Laser Scanner, Point Clouds, PSR with Envelope Constraints, Triangular Mesh

DOI: 10.14733/cadconfP.2025.205-210

Introduction:

Point clouds of large-scale scenes acquired by terrestrial laser scanners (TLS) are used in various fields, including plant, civil engineering, architecture, and surveying. The triangular meshes from point clouds increase the usability of scanned data for many geometric applications, such as various geometric calculations, simulations, and visualization. However, there are some challenges in generating high-quality mesh models for point clouds of large-scale environments with complex objects. Although many methods have been developed for mesh generation from point clouds, such as direct methods, implicit-based methods, and machine learning-based methods, which are summarized in [1,6,7], we focused on the Poisson surface reconstruction with envelope constraints (PSRE) [4] because of its ability for accurate surface generation under constraints for generated surfaces by envelope based on the space occupancy information. However, there is room for improvement in the accuracy of reconstructed surfaces and applicability to large-scale scenes. The objective of this study is to develop a quality mesh generation method using PSRE to TLS point clouds of large-scale scenes with complex objects such as engineering plants and production facilities. In this paper, we describe a hybrid strategy for efficient surface generation, space subdivision, and indicator function merging for managing the balance of keeping detailed shapes and interpolation for lack of points, and an envelope generation method with space subdivision for large-scale scenes.

Main idea:*Poisson Surface Reconstruction with Envelope Constraints and Method Overview*

Among the many mesh generation methods from point clouds [1,6,7], Poisson surface reconstruction (PSR) [3] is outstanding in the accuracy and interpolation of the generated mesh [6]. PSR is a method for fitting the gradient of the indicator function $\chi: R^3 \rightarrow R$, whose value is one inside the object and zero outside, to the normal vector field \mathbf{V} defined by the normals $\{\mathbf{n}_i\}$ of the input point set $\{\mathbf{p}_i \in R^3\}$. The indicator function is derived by solving the Poisson equation $\Delta\chi = \nabla \cdot \mathbf{V}$. Although PSR can produce quality surfaces interpolating the unscanned regions where points are lacking caused by the occlusion in 3D scanning, it often yields ballooning at the unscanned region, as shown in Fig. 1(a). Poisson surface reconstruction with envelope constraints (PSRE) [4], which is an extension of PSR, can generate more accurate meshes than the standard PSR. PSRE can avoid undesired ballooning by defining the envelope, which is a boundary of spatial regions where no object exists, as a Dirichlet boundary constraint on PSR, as shown in Fig. 1(b). In the 3D scanned space, the envelope is defined as the depth hull [2], which is the boundary between the occupied and free space in the 3D occupancy map in 3D scanning. However, in the application of PSRE to point clouds of large-scale scenes with complex objects, some issues were observed in terms of the inaccuracy of the generated mesh and

computational cost. To overcome these issues, some techniques for applying PSRE to point clouds of large-scale scenes with complex objects, such as plants and production facilities, are described in this paper. The first is to use a hybrid approach of implicit and region-based methods for efficient computation. The second is the point cloud subdivision and merging indicator functions for accurate surface reconstruction. The third is envelope generation for subdivided spaces to apply PSRE to subdivided point clouds of large-scale scenes.

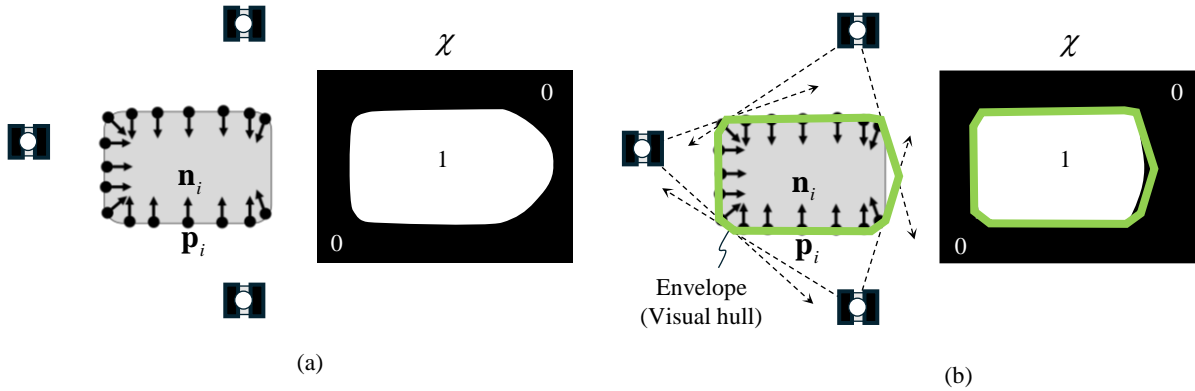


Fig. 1: Point clouds, normals, and indicator functions: (a) PSR and (b) PRSE.

Fig. 2 shows the proposed method. The inputs are registered point clouds $P_k = \{\mathbf{p}_i^k\}$ of multiple scans s_k ($k=1, \dots, M$). First, the proposed method structures the TLS point cloud for each scan using the regularity of TLS measurements for efficient point cloud processing (Fig. 2, A1). Then, a region-based method based on the region growing method with interpolation is used to generate meshes of planar regions (Fig. 2, A2). Next, point clouds are subdivided (Fig. 2, A3), and envelopes are generated for subdivided point clouds (Fig. 2, A4). PSRE is applied to each subdivided point cloud using the corresponding envelope (Fig. 2, A5). Point cloud subdivision for PSRE application is done for two different subdivision widths, and the resulting two indicator functions for detail preservation and interpolation are merged (Fig. 2, A6). Finally, the surface mesh is obtained by iso-surface extraction for merged functions (Fig. 2, A7).

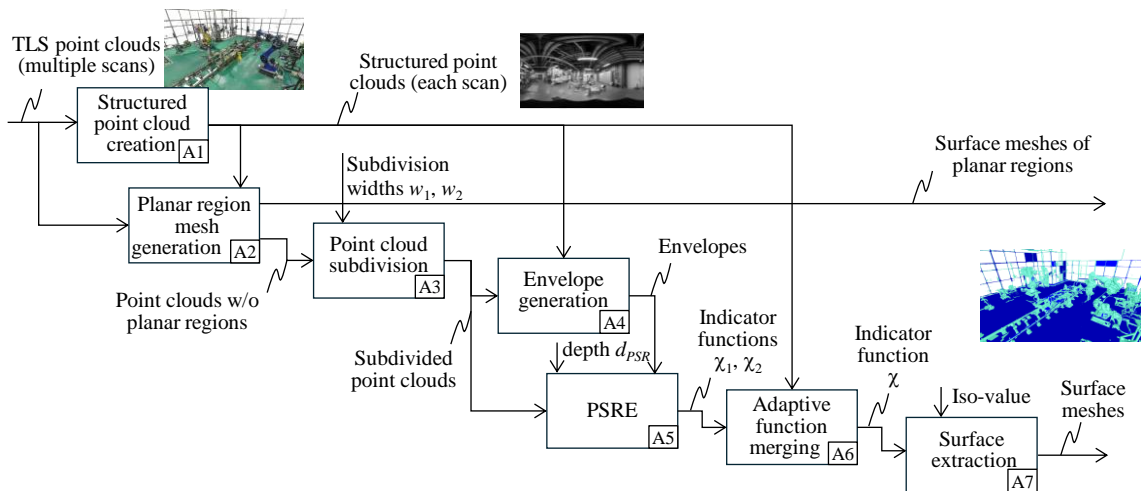


Fig. 2: Proposed method.

Structured Point Cloud Creation

In laser scanning using TLS, the laser is irradiated for directions determined by uniform angle intervals for azimuth $\Delta\theta$ and elevation angle $\Delta\phi$, as shown in Fig. 3. Therefore, the structured point cloud that is the 2D regular arrangement of points in the TLS point clouds of each scan can be obtained using two indices for azimuth and elevation angle [5]. This structure allows us to find neighbors of each point by a computational complexity of $O(1)$.

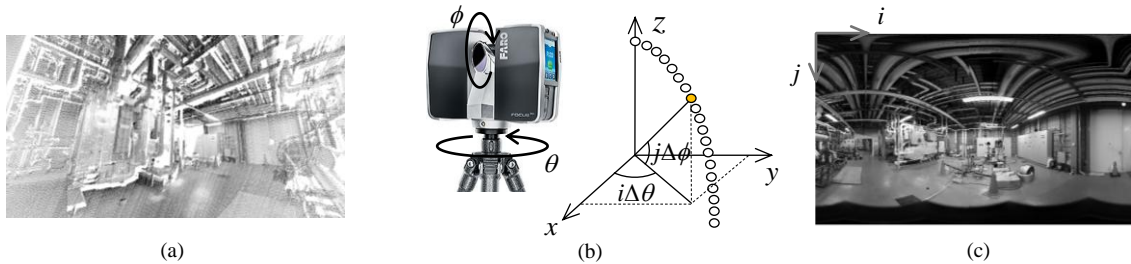


Fig. 3: Structured point cloud: (a) Point cloud, (b) Terrestrial laser scanner and laser irradiation angles, and (c) Structured point cloud.

Planar Region Mesh Generation

In large-scale scenes of engineering plants and production facilities, many large planes often exist. Region-based methods are suitable for mesh generation of planar regions in TLS point clouds [5]. Removing points on planar regions can drastically reduce the points for PSRE. It realizes efficient processing of PSRE and reduces the number of triangles of the resulting meshes. In our method, planar regions in each scan are first detected by region growing using structured point clouds. Then, the extracted co-planar regions of different scans are merged. The points of a merged planar region are projected onto the plane, and boundary point sequences are extracted using alpha shapes. The closed regions bounded by concave boundaries are occluded by the inner object. Therefore, the inner point sequences with concave boundaries are removed to reduce the number of triangles in the first meshes. Meshes are generated by constrained Delaunay triangulation.

Accurate and Interpolated Mesh Generation

PSRE defines the indicator function by a linear combination of hierarchical B-spline basis functions based on the octree [4], and the functions in coarser levels have an impact on the accuracy of the overall indicator function. This characteristic is particularly noticeable for large scenes, which tend to generate inaccurate smoother meshes. This problem can be solved by narrowing the support width in the coarser level by space subdivision. In our method, first, a uniform grid that covers the input point cloud is defined, and each face of the grid cell is offset outside to create overlaps between neighboring cells. As a result, a set of cells overlapping with neighboring cells is obtained. The local point clouds in each cell are extracted as the subdivided point clouds, and PSRE is applied to each subdivided point cloud. By creating overlaps, the gaps between meshes of neighboring cells are reduced.

The detail preservation and the degree of interpolation depend largely on the space subdivision width (cell size for subdivided point clouds). A smaller width produces a mesh with excellent detail preservation, while a larger width produces a mesh with excellent interpolation for lack of points. Therefore, two different widths w_1 and w_2 ($w_1 < w_2$) are used in our method. PSRE is applied to each subdivided point cloud, and two indicator functions χ_1 and χ_2 for w_1 and w_2 are obtained, as shown in Fig. 4(b) and 4(c). To achieve both detail preservation and interpolation, the functions are merged. In our method, χ_1 is adopted for the detailed region, and χ_2 is used for the other regions. In order to find the detailed region, the shape complexity c_i at each point i in the point clouds is estimated. In our implementation, c_i is the average of angle differences between the unit normal \mathbf{n}_i of point i and the unit normal \mathbf{n}_j of its neighbor points $j \in N_i$ on the structured point cloud, i.e.

$c_i = N_i^{-1} \sum_{j \in N_i} \cos^{-1}(\mathbf{n}_i \cdot \mathbf{n}_j)$. Then, if the ratio of points that satisfy $c_i > \tau_d$ in the octree cell for width w_i in PSRE is larger than a given threshold, its parent cell is marked as *detailed* (Fig. 4(d)). Next, a uniform grid with the same cell size for the octree leaf is created, and χ_1 is assigned to the grid point corresponding to the *detailed* cells and χ_2 is assigned to the one for the other cells using trilinear interpolation. Finally, the Gaussian filter is applied to the assigned values on the grid (Fig. 4(e)). Surface meshes are generated by applying the Marching cubes method to the resulting grid.

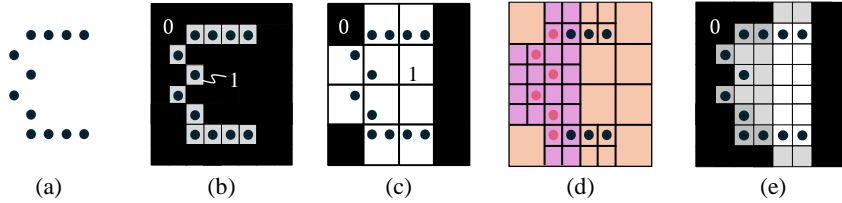


Fig. 4: Adaptive merging of the indicator function: (a) Point cloud, (b) Indicator function χ_1 for detailed region, (c) Indicator function χ_2 for interpolation, (d) Detailed regions in octree, and (e) The merged function.

Envelope Generation for Subdivided Point Clouds

The envelope can be defined as the boundary between occupied and free spaces of the 3D occupancy map obtained by ray casting from the scanner positions. However, if ray casting is applied directly to subdivided space S_i without consideration of occlusions by others, the incorrect envelope is generated as shown in Fig. 5(b). Therefore, in each S_i of the subdivided point clouds, the target of ray casting is restricted to the surfaces of S_i that are visible from each scanner, as shown in Fig. 5(c). In our method, the visible surfaces of S_i are efficiently detected by using a depth map for each scanner. The depth map $d_k(i, j)$ for each scan k is created from the structured points. Where i and j are indices corresponding to azimuth and elevation angles as shown in Fig. 3. Let $\mathbf{f}_k: R^3 \rightarrow N_0^2$ be a function that computes the indices (i, j) in the structured point cloud of scanner k from the three-dimensional point. The depth value is defined by $d_k(\mathbf{f}_k(\mathbf{R}_k^{-1}(\mathbf{p}_m^k - \mathbf{t}_k))) = \|\mathbf{R}_k^{-1}(\mathbf{p}_m^k - \mathbf{t}_k)\|$, where \mathbf{R}_k and \mathbf{t}_k are the rotation matrix and the translation vector (scanner's position) of registration of scanner k . Using the depth map, point \mathbf{c} that is visible from scanner k satisfies $\|\mathbf{c} - \mathbf{t}_k\| < d_k(\mathbf{f}_k(\mathbf{R}_k^{-1}(\mathbf{c} - \mathbf{t}_k)))$, as shown in Fig. 5(d).

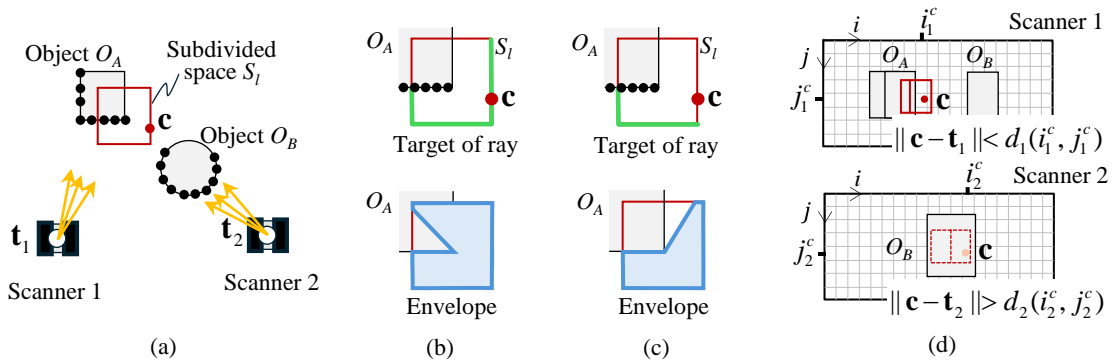


Fig. 5: Envelope generation for a subdivided space: (a) A scene with objects and scanners, (b) Envelope without consideration of occlusions, (c) Envelope with consideration of occlusions, and (d) Depth test on the structured point cloud.

In envelope creation, a voxel grid is defined for the subdivided space, and a set of visible center positions of surface cells is obtained using the visibility test described above. Then, a space occupancy map is created by ray casting from scanner k to visible surface cells. The visibility test and ray casting

are done for all scanners, and the envelop mesh is generated by marching cubes for the resulting occupancy map.

Results

The proposed method was applied to the six-scan TLS point clouds (about 84 million points) of the factory, as shown in Fig. 6(a). In Fig. 6(b), meshes from the region-based method are shown in blue, and the meshes from PSRE are in green. The region-based method extracted 80% of the 84 million points as planar regions. The number of planar regions was 386. Figs. 6(d)-(f) show the meshes by PSR, PSR with space subdivision, and PSRE with space subdivision (w/o function merging) for point clouds of a robot shown in Fig. 6(c). From Fig.6(e), it is observed that the point cloud subdivision reduces excessive interpolation at concave parts of links with global PSR application (Fig.6(d)). In addition, using envelope constraints, the accuracy of meshes is drastically improved, and meshes that are visually almost similar to the point clouds were obtained. The total computation time for mesh generation was 12 minutes on a PC with a Ryzen3900X CPU, and the total number of triangles was approximately 10 million. By using the region-based method, the computation time and total number of triangles were reduced by 10% and 20%, respectively.

Fig. 7 shows the effectiveness of the indicator function merging at the detailed shape of wire harnesses and the large lack of points. Fig.7(a) shows the point clouds, and Fig. 7(b) shows the meshes generated by an indicator function χ_1 of a small subdivision space width w_1 . The detailed shapes are reconstructed well (top figure). However, inaccurate surfaces are obtained for the lack of points due to the low degree of interpolation. On the other hand, Fig.7(c) shows the meshes for a large space subdivision width w_2 . Better interpolation is achieved for a lack of points, but too much for detailed shapes. Fig.7(d) shows the mesh from the indicator function merging by our method. In the results, our method achieves good properties for both detailed shape preservation and interpolation for a large lack of points. Subdivision widths w_1 and w_2 are determined experimentally and set to 1m and 2m. By using the function merging, computation times of mesh generation for a subdivided space were increased from about 30 seconds to 3~4 minutes. In particular, Gaussian filtering and color interpolation were time-consuming. Since there was no ground truth for the target geometry, the evaluation of the generated meshes was limited to a visual evaluation. Detailed accuracy evaluation and shortening the computation times were included in future works.

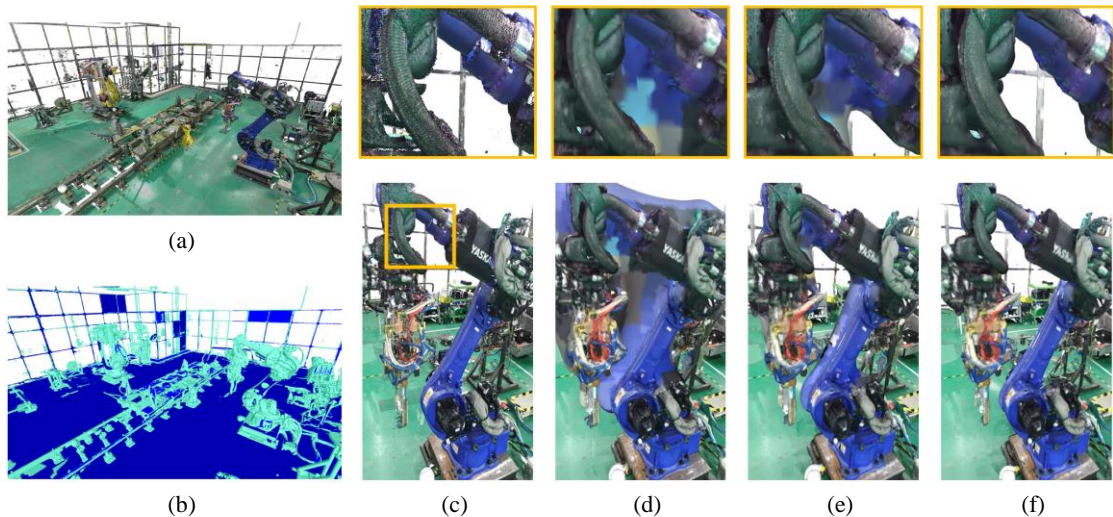


Fig. 6: Used point cloud and resulting meshes: (a) Point cloud for experiments, (b) Planar region meshes (green) and PSRE meshes (blue), (c) Point clouds of a robot, (d) PSR mesh, (e) PSR mesh with space subdivision, and (f) PSRE mesh with space subdivision.

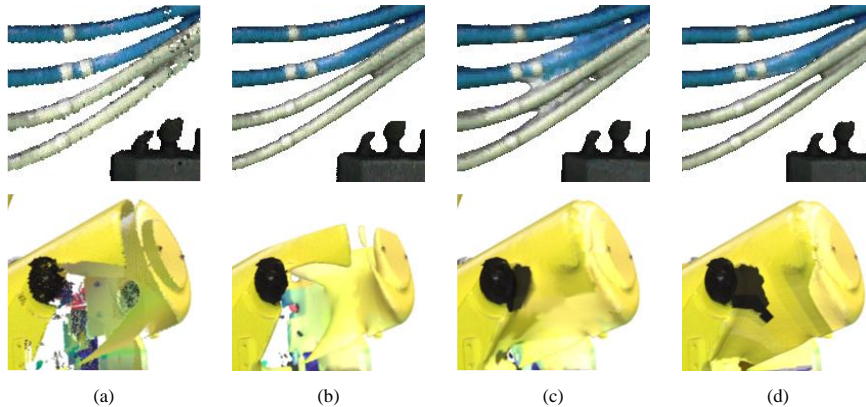


Fig. 7: Effectiveness of indicator function merging at detailed shape (top) and lack of points (bottom): (a) Point clouds, (b) Meshes from smaller subdivision width w_1 , (c) Meshes from larger subdivision width w_2 , and (d) Meshes from function merging.

Conclusions:

A method for generating accurate triangular meshes from TLS point clouds of scenes with complex objects using Poisson surface reconstruction with envelope constraints (PSRE) was proposed. The method consists of planar-region mesh generation for efficient processing, space subdivision and indicator function merging for detail preservation and interpolation, and envelope generation for subdivided spaces in order to apply PSRE to point clouds of the large-scale scene. The experiments for TLS point clouds of a factory showed that our method enables the application of PSRE to TLS point clouds of large-scale scenes with complex objects and generates better meshes in the sense of detail preservation and interpolation for lack of points. Improving the computational efficiency and detailed accuracy evaluation of the resulting meshes is included in future work.

Daiki Koyama, <https://orcid.org/0009-0005-3110-1773>

Hiroaki Date, <https://orcid.org/0000-0002-6189-2044>

Satoshi Kanai, <https://orcid.org/0000-0003-3570-1782>

References:

- [1] Berger, M.; Tagliasacchi, A.; Seversky, L. M.: A Survey of Surface Reconstruction from Point Clouds, *Computer Graphics Forum*, 36(1), 2017, 301-329.
- [2] Bogomjakov, A.; Gotsman, C.; Magnor, M.: Free-viewpoint video from depth cameras, *Proceedings of the Vision, Modeling and Visualization*, 2006, 89-96.
- [3] Kazhdan, M.; Bolitho, M.; Hoppe, H.: Poisson Surface Reconstruction, *Proceedings of the 4th Eurographics Symposium on Geometry Processing*, 2006, 61- 70.
- [4] Kazhdan, M.; Chuang, M.; Rusinkiewicz, S.; Hoppe, H.: Poisson Surface Reconstruction with Envelope Constraints, *Computer Graphics Forum*, 39(5), 2020, 173-182. <https://doi.org/10.1111/cgf.14077>
- [5] Masuda, H.; Niwa, T.; Tanaka, I.: Reconstruction of Polygonal Faces from Large-Scale Point Clouds of Engineering Plants, *Computer-Aided Design & Applications*, 12(5), 2015, 555-563. <https://doi.org/10.1080/16864360.2015.1014733>
- [6] Sulzer, R.; Marlet, R.; Vallet, B.; Landrieu, L.: A Survey and Benchmark of Automatic Surface Reconstruction from Point Clouds, *IEEE Transactions on Pattern Analysis and Machine Intelligence*, 47, 2025, 2000-2019. <https://doi.org/10.1109/TPAMI.2024.3510932>
- [7] You, C. C.; Lim, S. P.; Lim, S. C.; Tan, S. T.; Lee, C. K.; Khaw, Y. M. J.: A Survey on Surface Reconstruction Techniques for Structured and Unstructured Data, *IEEE Conference on Open Systems*, 2020, 37-42.